

BIMODAL PORE SIZE MESOPOROUS MCM-48 PREPARED BY POST-SYNTHESIS ALUMINATION

Lau Chin Guan, Hadi Nur* and Salasiah Endud

Ibnu Sina Institute for Fundamental Science Studies
Universiti Teknologi Malaysia
81310 UTM Skudai, Johor, Malaysia

*Corresponding author: hadi@kimia.fs.utm.my

Abstract: *Synthesis of mesoporous materials with a bimodal pore size has always been of great importance for size-selective separation process. Especially, ordered mesoporous cubic MCM-48 with its highly interwoven and branched pore structure, is a potential separation material in applications similar to which zeolites are now being used. This material could have specific technological advantages because of the 3-D channel network of MCM-48. We report that by post-synthesis alumination of siliceous MCM-48 containing organic templates with sodium aluminate solution, a bimodal pore size of MCM-48 is obtained. In particular, it was found from N₂ adsorption–desorption measurements that MCM-48 obtained had 26 Å and 38 Å dual narrow pore size distributions. From ²⁷Al solid-state MAS NMR measurements, it is confirmed that the aluminium is in the framework structure of mesoporous MCM-48.*

Keywords: MCM-48, bimodal pore size mesoporous aluminosilicate

Abstrak: *Sintesis bahan mesolintang dengan saiz liang dwimodal sangat berguna untuk proses pemisahan selektif berdasarkan ukuran. Terutamanya untuk mesolintang MCM-48 yang berbentuk kiub dengan struktur liang yang saling berhubungan dan bercabang, yang berpotensi sebagai bahan pemisah dalam aplikasi yang sama seperti zeolit digunakan sekarang. Disebabkan saluran jaringan 3 dimensi bagi MCM-48, bahan ini mungkin mempunyai kelebihan teknologi yang khusus. Kami melaporkan bahawa pengaluminiuman pasca sintesis bagi MCM-48 yang mengandungi templat organik dengan larutan natrium aluminat, liang dwimodal bagi MCM-48 diperolehi. Khususnya, didapati daripada pengukuran penjerapan-penyahjerapan N₂, bahawa MCM-48 mempunyai taburan saiz liang yang sempit, 26 Å dan 38 Å. Daripada pengukuran ²⁷Al MAS NMR keadaan pepejal dapat disahkan bahawa aluminium berada di dalam struktur bingkai mesolintang MCM-48.*

Kata kunci: MCM-48, mesolintang aluminosilikat saiz liang dwimodel

1. INTRODUCTION

Since the discovery of the first ordered mesoporous materials, denoted as M41S family, a new class of molecular sieves exhibiting ordered arrangement of large pores with uniform cross-sectional diameter in the range 20–100 Å has been generated.¹ Among these materials, the two most investigated are MCM-41 with a hexagonal array and MCM-48 with a bicontinuous *Ia3d* cubic pore system. The discovery of these materials has catalyzed enormous research activities of various fields including catalysis² and membrane³. Recently, ordered mesoporous inorganic membranes with uniform pores have been of great interest for separation processes because of their high stability under severe conditions such as at high temperature and in organic solvent.^{4,5} On the other hand, in the separation of more bulky organic molecules, mesoporous membranes are promising materials to obtain high flux properties. For these applications, the texture and morphology of the mesoporous materials become crucial parameters in fulfilling the desired purposes.

Currently, bimodal or multimodal of pore system have attracted great attention because it will enhance the mass transfer kinetics and possesses high loadability, which are important features for adsorbents employed in separation techniques.⁶⁻⁹ The larger pores enable high mass transfer due to connective flow, while the smaller pores are responsible for the high surface areas of these materials and therefore enable high capacity for potentially adsorbed molecules. Here, we report the first attempt of the preparation of MCM-48 with a bimodal pore size structure by post synthesis alumination.

2. EXPERIMENTAL

2.1 Synthesis

Pure siliceous (Si-MCM-48) and Al-MCM-48 have been synthesized via a mixed cationic-neutral templating route using the cationic cetyltrimethylammonium bromide (CTABr) and neutral Triton X-100 (TX-100) surfactants.^{10,11} Rice husk ash (RHA), obtained from an open burning site was used as the silica source. A typical synthesis proceeds as follows. Firstly, the sodium silicate was prepared by combining 4 g RHA with 1 g NaOH and 35 g H₂O. The mixture was then stirred for 2 h at 353 K. The mixture was then cooled to room temperature. The surfactant mixture was prepared by heating 3.87 g CTABr and 1.17 g TX-100 simultaneously in 55 g of H₂O. The surfactant solution was then cooled to room temperature. The sodium silicate solution and the surfactant solution were simultaneously poured into a 125 mL polypropylene bottle and shaken vigorously for 30 minutes. The gel mixture thus obtained was

subsequently heated under static conditions at 370 K for two days in order to form the surfactant–silica mesophases. The molar composition of the final gel mixture was 5 SiO₂ : 1.25 Na₂O : 0.15 TX-100 : 0.85 CTABr : 400 H₂O. The pH of the mixture was then adjusted to 10.2. The reaction mixture was again heated for two more days following the pH adjustment. For siliceous MCM-48, solid products from the reaction mixture were recovered and washed with double distilled water (1 L). Al-MCM-48 with various Si/Al ratios (Si/Al = 20, 30, 50 and 100) were synthesized by adding appropriate amount of aqueous solutions of sodium aluminate (5 wt%) to the mixture after pH adjustment and heated further for 7 days. To remove the surfactant templates, the as-synthesized sample was calcined in air under static conditions at 823 K for 6 h, with a linear temperature ramp of 1 K/min and two plateaus of 60 minutes each at 423 K and 623 K, respectively.

2.2 Characterizations

Powder X-ray diffraction patterns of MCM-48 samples were measured on Bruker D8 Advance diffractometer with Cu-K_α radiation (40 KV, 40 mA) at 0.01° step size and 1 s step time over a 1.5° < 2θ < 10° range. The samples were prepared as thin layers on glass slides. The BET surface areas of calcined Si-MCM-48 and Al-MCM-48 were measured using Micromeritics ASAP 2010 apparatus. Prior to adsorption, the samples were outgassed for 2 h at 473 K under vacuum. Solid state ²⁷Al MAS NMR spectra were measured using a Bruker Ultrashield 400 instrument at 104.2 MHz, spinning at 7000 Hz, 1.9 μsec pulses and 2 s relaxation time delays. Each spectrum was obtained with 6000 scans. The chemical shifts of ²⁷Al were reported relative to Al(H₂O)₆³⁺ as the reference.

3. RESULTS AND DISCUSSION

Figures 1(a) and 1(b) show the XRD patterns of as-synthesized and calcined samples for sample Si-MCM-48 and aluminated samples Al-MCM-48 respectively. For the Si-MCM-48, a sharp d₂₁₁ Bragg reflection, a weak d₂₂₀ Bragg reflection shoulder, and several unresolved peaks between 2θ = 3.5°–5.5° are observed. The XRD pattern is similar to *Ia3d* bicontinuous cubic phase, which can be classified as typical for MCM-48 material.¹² The XRD data gives the evidence that the highly ordered pore system of siliceous cubic MCM-48 material has been formed completely after the hydrothermal treatment. As for Al-MCM-48 with various Si/Al ratios, the XRD patterns are similar to that of Si-MCM-48, suggesting that no structural change after introduction of aluminium source. The results of the XRD analyses of the samples are listed in Table 1. It is noted that the cubic unit cell parameter of Al-MCM-48 samples are similar to

that of Si-MCM-48 sample, revealing that incorporation of aluminium into the mesostructure of MCM-48 by post synthesis alumination method does not affect the ordered structure of the mesophases.

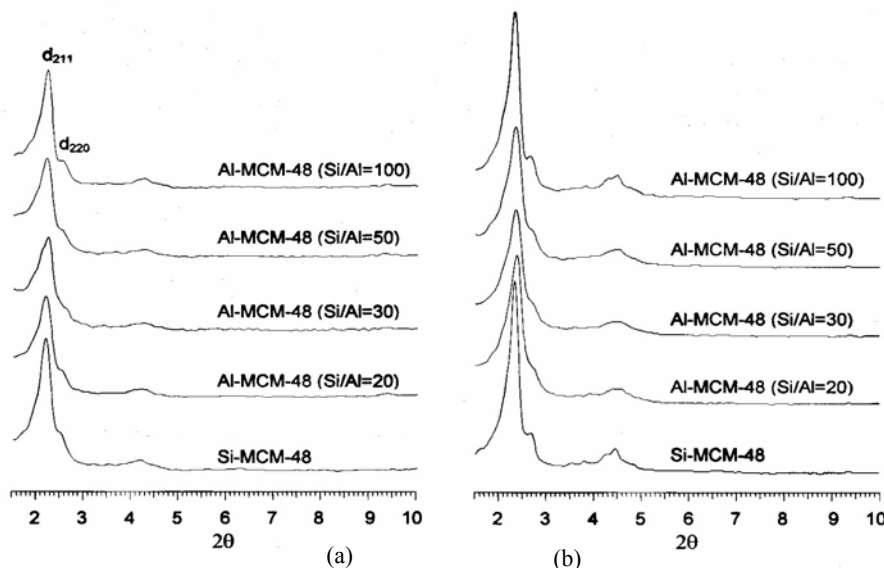


Figure 1: XRD patterns of the (a) as-synthesized and (b) calcined MCM-48 samples.

Table 1: XRD analysis results of Si-MCM-48 and Al-MCM-48 samples.

Samples	d_{211} spacing / Å		Unit cell parameter ^a / Å		contraction / %
	as-synthesized	calcined	as-synthesized	calcined	
Si-MCM-48	40.59	38.77	99.4	95.0	4.4
Al-MCM-48 (Si/Al=20)	39.98	37.18	97.9	91.1	6.9
Al-MCM-48 (Si/Al=30)	39.70	37.38	97.3	91.2	6.3
Al-MCM-48 (Si/Al=50)	39.94	37.49	97.8	91.8	6.1
Al-MCM-48 (Si/Al=100)	39.90	37.86	97.7	92.7	5.1

^aCubic unit cell parameter calculated as $a_0 = d_{211}\sqrt{6}$.

Figure 2 shows the nitrogen adsorption-desorption isotherms for calcined samples and their corresponding pore size distribution curves calculated using the BJH method¹³ based on the desorption branch. The obtained isotherms demonstrated that all of the samples display the typical irreversible type IV adsorption isotherm with H3 hysteresis loop, as identified by IUPAC.¹⁴ These results suggest that the samples possess slit-shaped mesopores. However, it is noted that the hysteresis loops of aluminium containing MCM-48 are larger and more definite than Si-MCM-48. This suggests that the porosity of aluminium containing MCM-48 is different from Si-MCM-48.

Further investigation of the isotherms show that the desorption isotherm branch of the Si-MCM-48 exhibits one sharp inflection, characteristic of capillary condensation at relative pressures of $0.30 < P/P_0 < 0.36$, whereas aluminium containing MCM-48 exhibits two sharp inflections characteristic of capillary condensation at relative pressures of $0.30 < P/P_0 < 0.36$ and $0.47 < P/P_0 < 0.50$. Hence, it illustrates that the pore size distribution of Si-MCM-48 is clustered around one pore size and that of aluminium containing MCM-48 around two pore sizes. From the plot of pore size distribution curves (Fig. 2), it is confirmed that Si-MCM-48 only possesses a well-defined pore size distribution centered around 26 Å, whereas the aluminium containing MCM-48 have two distinguishable pore size distributions centered around 26 Å and 38 Å. It is noted that the amount of the larger mesopore (38 Å) increases parallel with the increase of aluminium content, indicating that the aluminium plays an important role in formation of these mesopores. Therefore, it gives the evidence that the bimodal pore structure of Al-MCM-48 mesoporous materials have been created during the post synthesis alumination.

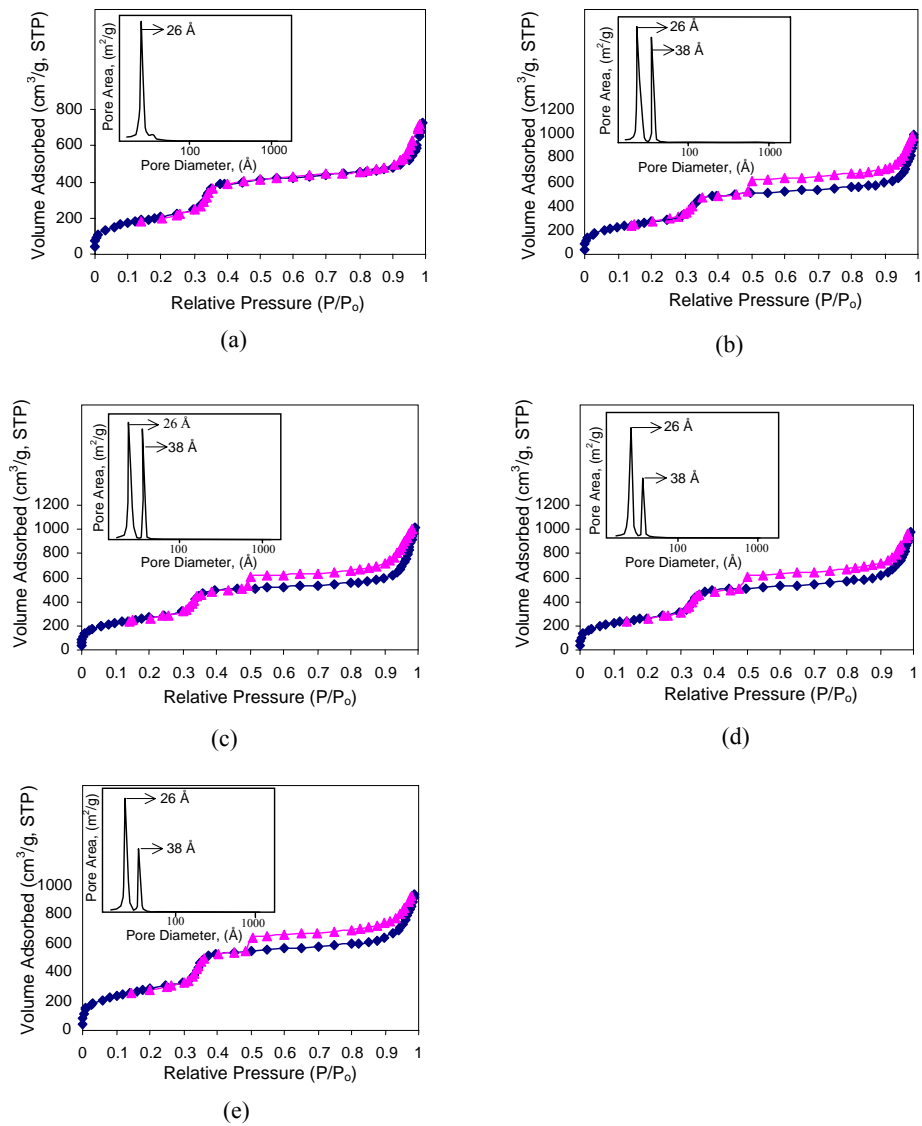


Figure 2: N_2 adsorption-desorption isotherms (— \blacklozenge —) adsorption, (— \blacktriangle —) desorption of calcined samples and its corresponding pore size distribution curve (inset): (a) Si-MCM-48, (b) Al-MCM-48 (Si/Al = 20), (c) Al-MCM-48 (Si/Al = 30), (d) Al-MCM-48 (Si/Al = 50), and (e) Al-MCM-48 (Si/Al = 100).

Table 2 shows the surface properties for Si-MCM-48 and Al-MCM-48. It can be seen that all samples possess high BET surface areas and the values are not significantly different from each other. Therefore, it can be concluded that the addition of aluminium did not influence the surface areas. However, the pore volume of aluminium containing MCM-48 mesoporous materials is much higher than Si-MCM-48. The pore volume increases around 29% – 39% after the addition of aluminium. The increase of pore volume may be due to the larger pores that was created by aluminium.

Table 2: Surface properties for Si-MCM-48 and Al-MCM-48.

Samples	BET surface area / $\text{m}^2 \text{g}^{-1}$	Pore diameter / Å	Total Pore volume / $\text{cm}^3 \text{g}^{-1}$	Increase of pore volume / %
Si-MCM-48	1058	26	1.17	–
Al-MCM-48 (Si/Al = 20)	991	26 and 38	1.58	35
Al-MCM-48 (Si/Al = 30)	983	26 and 38	1.63	39
Al-MCM-48 (Si/Al = 50)	975	26 and 38	1.56	33
Al-MCM-48 (Si/Al = 100)	1043	26 and 38	1.51	29

^aThe percentage increase of pore volume is calculated based on pore volume of siliceous MCM-48.

Based on the above results, it can be proposed that aluminium containing MCM-48 possessing hierarchical mesoporosity, are made up of two types of porous system, ordered bicontinuous $Ia3d$ cubic and narrow but with irregular arrangement of pore system. The nitrogen adsorption-desorption analyses show that the aluminium containing materials exhibit dual narrow pore size distributions. Nevertheless, the XRD diffractograms only show bicontinuous $Ia3d$ cubic diffraction pattern and no overlapping of Bragg diffraction peaks has been detected. It is known that only regular arrangement of mesoporous pore system will give the Bragg diffraction peak, and hence an irregular pore system will not contribute to any diffraction peak at low 2θ angle. Therefore, from XRD result it can be concluded that the pore size distribution centered at 26 Å is due to the bicontinuous $Ia3d$ cubic pore system. It is supported by the fact that the contraction of the unit cell of Al-MCM-48 samples are similar to that of

Si-MCM-48 (see Table 1). Whilst, the pore size distribution centered at 38 Å is attributed to irregular but narrow pore system. The Al-MCM-48 mesoporous materials with a controlled interconnected hierarchical pore system are excellent candidates as membrane for separation processes. This is due to the fact that interconnected hierarchical pore system will significantly enhance mass transfer of compounds to the adsorption sites within the packing materials.⁹

Figure 3 depicts the ²⁷Al MAS NMR spectra of aluminium containing MCM-48 samples. ²⁷Al MAS NMR of the aluminium containing samples are similar, solitarily exhibits an intense peak at 50 ppm, assigned to tetrahedrally coordinated Al which is incorporated into the framework structure of MCM-48. It implies that aluminium takes part in constructing the irregular but narrow pore system. Although a novel bimodal pore structure MCM-48 has been successfully synthesized by post synthesis alumination, the mechanism of the formation of secondary pores is not well understood. These pores are probably created by adjoining of the primary particles and followed by random cross-linking between these particles in the presence of aluminium. Based on the pore distribution curve and ²⁷Al MAS NMR results, the degree of cross-linking seems to be related to the aluminium content. The formation of this type of secondary mesopores was found to occur only in the gel mixture, probably due to the presence of aluminosilicate ion, which facilitates the cross-linking process. Another possibility of the formation of secondary mesopore may be due to the presence of template based on liquid-crystal templating (LCT) mechanism. One expects that the formation of secondary mesopore is more probable since the LCT mechanism involved the dissolution and the self assembling of surfactant species which may cause the collapsing of the structure of MCM-48.

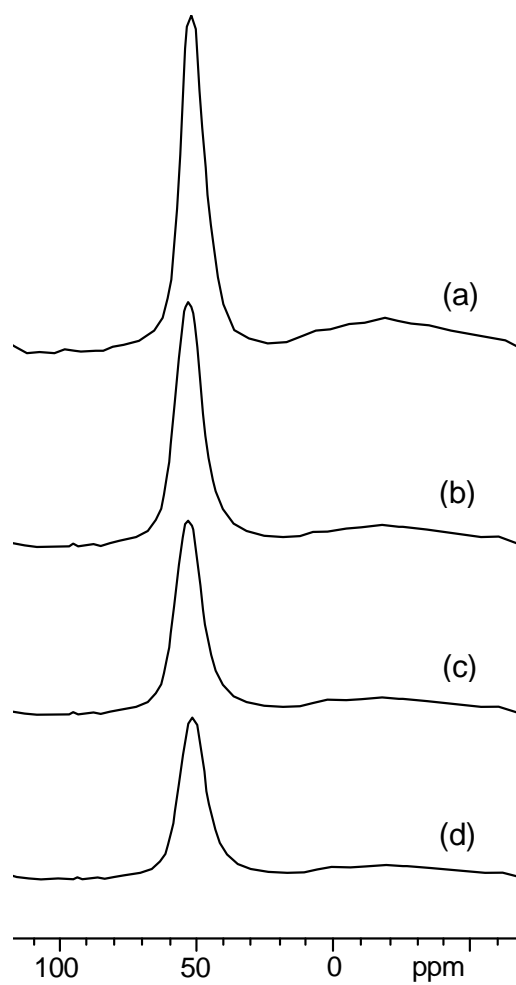


Figure 3: ^{27}Al MAS NMR spectra of aluminium containing MCM-48 samples with Si/Al are (a) 20, (b) 30, (c) 50, and (d) 100.

4. CONCLUSION

Bimodal mesoporous aluminium containing MCM-48 with interconnected hierarchical structure has been synthesized through post synthesis alumination method. Two types of pore systems, ordered bicontinuous *Ia3d* cubic MCM-48 pore system and narrow but irregular pore system centered at 26 Å and 38 Å, have been generated. The formation of secondary mesopores during the post synthesis alumination has been attributed to the presence of aluminosilicate ion.

5. ACKNOWLEDGEMENT

This research was supported by IRPA SR 0005/09-04 from the Ministry of Science, Technology and Environment (MOSTE), Malaysia.

6. REFERENCES

1. Beck, J.S., Vartuli, J.C., Roth, W.J., Leonowics, M.E., Kresge, C.T., Schmitt, K.D., Chu, C.T.-W., Olson, D.H., Sheppard, E.W., McCullen, S.B., Higgins, J.B. and Schlenker, J.L. 1992. A new family of mesoporous molecular sieves prepared with liquid crystal templates. *J. Am. Chem. Soc.* 114: 10834–10843.
2. Corma, A. 1997. From microporous to mesoporous molecular sieve materials and their use in catalysis. *Chem. Rev.*, 97: 2373–2420.
3. Nishiyama, N., Park, D.H., Koide, A., Egashira, Y. and Ueyama, K. 2001. A mesoporous silica (MCM-48) membrane: preparation and characterization *J. Membrane Sci.*, 182: 235–244.
4. Gavalas, G.R., Megiris, C.E. and Nam, S.W. 1989. Deposition of H₂-permselective SiO₂ films. *Chem. Eng. Sci.*, 44: 1829–1835.
5. Tsapatsis, M., Kim, S., Nam, S.W. and Gavalas, G. 1991. Synthesis of hydrogen permselective silicon dioxide, titanium dioxide, aluminum oxide, and boron oxide membranes from the chloride precursors. *Ind. Eng. Chem. Res.*, 30: 2152–2159.

6. Yuan, Z.Y., Wang, J.Z., Zhang, Z.L., Chen, T.H. and Li, H.X. (2001). Vanadium- and chromium-containing mesoporous MCM-41 molecular sieves with hierarchical structure. *Microporous Mesoporous Mater.*, 43, 227–236.
7. Sun, J.H., Shan, Z., Maschmeyer, T. and Coppens, M.O. 2003. Synthesis of bimodal nanostructured silicas with independently controlled small and large mesopore sizes. *Langmuir*. 19: 8395–8402.
8. Grimes, B.A., Ludtke, S., Unger, K.K. and Liapis, A.I. 2002. Novel general expressions that describe the behavior of the height equivalent of a theoretical plate in chromatographic systems involving electrically-driven and pressure-driven flows. *Chromatogr. A* 979: 447–466.
9. Liapis, A.I., Meyers, J.J. and Crosser, O.K. 1999. Modeling and simulation of the dynamic behavior of monoliths: Effects of pore structure from pore network model analysis and comparison with columns packed with porous spherical particles. *J. Chromatogr. A*. 865: 13–25.
10. Ryoo, R., Joo, S.H. and Kim, J.M. 2004. Energetically favored formation of MCM-48 from cationic-neutral surfactant mixtures. *J. Phys. Chem. B*. 103: 7435–7440.
11. Nur, H., Lau, C.G., Endud, S. and Hamdan, H. 2004. Quantitative measurement of a mixture of mesophases cubic MCM-48 and hexagonal MCM-41 by ^{13}C CP/MAS NMR. *Mater. Lett.* 58: 1971–1974
12. Kresge, C.G., Leonowics, M.E., Roth, W.J., Vartuli, J.C. and Beck, J.S. 1992. Ordered mesoporous molecular sieves synthesized by a liquid-crystal template mechanism. *Nature* 359: 710–712.
13. Barrett, E.P., Joyner, L.G. and Halenda, P.P. 1951. The Determination of Pore Volume and Area Distributions in Porous Substances. I. Computations from Nitrogen Isotherms *J. Am. Chem. Soc.* 73: 373–380.
14. Leofanti, G., Padovan, M., Tozzola, G. and Venturelli, B. 1998. Surface area and pore texture of catalysts. *Catal. Today* 41: 207–219.